



Non-Singular Terminal Sliding Mode Control of a Nonholonomic Wheeled Mobile Robots Using Fuzzy Based Tyre Force Estimator

Foudil Abdessemed^{a,*}

^aDept. of Electronics, Faculty of technology, Batna University, Batna- 05000- Algeria, Email: f.abdessemed@univ-batna2.dz

ARTICLE INFO

Article history:

Received: 19 February, 2018

Received in revised form:

9 April, 2018

Accepted: 30 June, 2018

Keywords:

WMR, Slip
Fuzzy estimator
TSMC
Tyre forces

ABSTRACT

This paper, proposes a methodology to implement a suitable nonsingular terminal sliding mode controller associated with the output feedback control to achieve a successful trajectory tracking of a non-holonomic wheeled mobile robot in presence of longitudinal and lateral slip accompanied. This implementation offers a relatively faster and high precision tracking performance. We investigate this approach and demonstrate its feasibility for such situations where robustness against perturbation and measurement errors are required. In this study, tyre-forces are considered as perturbation. These forces appear because of wheel slip of the wheeled mobile robot moving at high speed or on a slippery surface. The need to compensate these forces are achieved through a design of an intelligent estimation paradigm. The estimator is realized by a fuzzy logic model that requires slip angle and slip ratio as inputs. The weight of the robot mechanical structure is an important parameter in this design. In fact, it is used to adjust the gain of the output, resulting in a fuzzy estimator that synthesizes the magic formula for a large model of tyres. Simulation results are reported and discussed.

1. Introduction

Outdoor wheeled mobile robot (WMR) navigation has stood as an open and challenging problem over decades. This is because an autonomous mobile robot must be able to operate in an unstructured environment and deal with its dynamic changes. Despite the

number of significant results obtained in this field, people still look for better solutions for faster mobile robots. Nonholonomic mobile robot are subjected to the nonholonomic constraint and generally navigate in environments cluttered with obstacles. Since the non-holonomic constraint makes path

planning more difficult [1], many techniques have been proposed to plan and generate paths [2, 3]. Moreover, the kinematic constraint is the other problem that can face trajectory planning. This can make time derivatives of some configuration variables non-integrable and hence, a collision free path in the configuration space may not be achieved by steering control [4]. In the past decades, people have tried different schemes of control laws, adapted to cope with these problems. Nonlinear control technique, for mobile robots, represented an alternative design method for control of the unknown nonlinear systems. The proposed control laws could compensate the effects of the nonlinearities under parametric uncertainties [5, 6]. In [7], Sarkar investigated the nonholonomy problem and suggested a control algorithm while assuming no-slip constraint at the contact point between the wheel and the ground surface. His work was the basis of many other contributions (e.g., [8]). However, feedback linearization does not allow stabilizing the mobile robot to a fixed position. On the other hand, the effect of parameter uncertainties and disturbances may result in unpredictable results. Moreover, for mobile robots operating at high speed and/or in unstructured environment, the assumption of a pure rolling does not hold and consequently slip constraints are no more negligible. In this case, performance degradations may be observed if the controller is not properly designed. These limitations conducted researchers to think of using other approaches. Variable structure theory [9-11] and its associated sliding mode behaviour have been considered as an excellent robust candidate approaches to control mobile robots subjected to parameter changes and disturbances. When the system uncertainties and external disturbances are bounded, conventional sliding mode control can guarantee stability and provides the required performances. However, with this control scheme, equilibrium point cannot be reached in a finite time. To overcome this problem, terminal sliding mode control

(TSMC) is proposed [12-15]. Nevertheless, still with this improved sliding mode control, one can face two disadvantages. The first is the existence of a singularity point problem. The second is the requirement for any compensation that comes from any drift when the ideal no slip assumption does not hold true. The non-singular terminal sliding mode control proposed in [16-22] solves the first issue. The second issue is raised when we need to include slip into the dynamic of the system. This relaxes the assumption of the pure rolling and approach the motion of the WMR to the pure reality. In the literature, few studies, related to this topic, have been investigated. One of the earliest paper that considered wheel slip as an important aspect can be found in [23], where a model has been derived considering the adhesion coefficient between the wheels of the robot and the surface as a function of the wheel slip. Many other works considered this issue unavoidable and arrived in publishing important results [24-27].

The main contributions of this paper are summarized as below:

- i. We included the slip and the skidding of the wheels into the dynamic model of the WMR such that it can be modeled as a perturbed model.
- ii. According to that, a fuzzy logic based estimator is designed on the basis of a known curves obtained by the well-known magic formula and generalized to a broad range of tyres through the WMR weight based gain.
- iii. The basic idea of finding the control law is to transform partially the system into a linear system. Inspired by the work of Feng *et al* [18], we propose a robust controller based on a non-singular terminal sliding mode control

The fuzzy estimator is inserted in the forward loop and serves in estimating the forces resulting from longitudinal and lateral wheel slip to anticipate the required compensation. The inputs of the fuzzy estimator are the slip

ratio and the slip angle. Their values are supposed to be available through adequate equipment measurements. One of the few attempts found in the literature is the work of Jayachandran *et al* [28]. However, their work is limited merely in comparing the results obtained, for one specific type of tyre, with the magic formula. To the best of our knowledge, our proposed approach is considered as a new contribution. Actually, the uncertain dynamics including uncertain parameters between tire force and tire slip are difficult to model accurately, which will limit the performance of model-based control methods. Generally, these parameters are obtained through experience for each type of tyre. Fuzzy logic provides a mathematical framework to deal with uncertainties inherently contained in input data and its associated membership functions.

The remainder of this paper is organized as follows. In section 2 we elaborate the kinematic and dynamic models of the nonholonomic wheeled mobile robot, section 3 presents the non-singular finite time sliding mode control for the dynamical model obtained in section 2. In section 4, we present the fuzzy logic based approach for estimating the tyre forces for different slip ratios and slip angles. Section 6 provides simulation results and section 7 concludes the paper.

2. Kinematics and Dynamic Model Elaboration of the WMR

2.1 Kinematic model

The model of the WMR is presented in Fig. 1. The model takes into account the two diametrically opposed drive wheels of radius r , the distance between the wheels is $2b$ and the right and left angular speeds of the drive wheels are successively ω_R and ω_L .

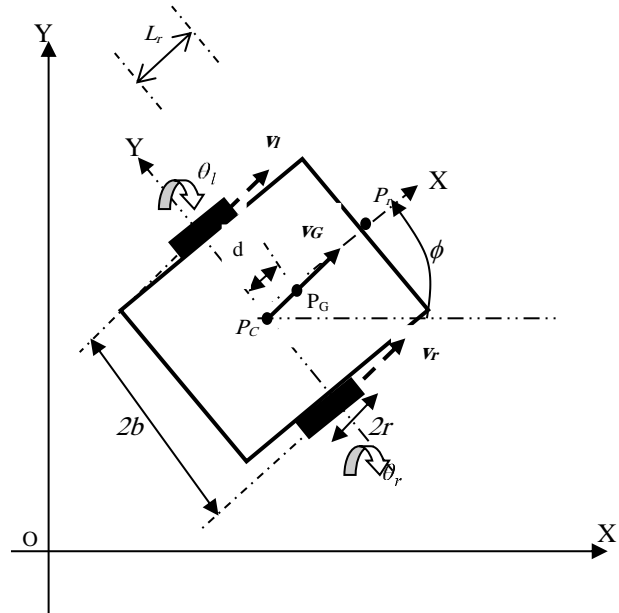


Fig 1. WMR configuration

The configuration of the wheeled mobile robot is $(x_G, y_G, \phi)^T$, (Fig. 1), where x_G and y_G represent the center of mass of the robot and ϕ its orientation with respect to the inertial frame. We consider the center of mass at point G distant from the origin C of the robot coordinate system by a distance d . The coordinates of points G and C are (x_C, y_C) and (x_G, y_G) respectively.

2.2 Dynamic modeling of the WMR subject to longitudinal and lateral slips.

In this section, the assumption of pure rolling and zero lateral slips is not considered. Therefore, the new dynamic model is more realistic and introduces the longitudinal as well as the lateral slips. The generalized coordinate q vector introduces the new state variables that are related to slippery and defined as ξ_i and η_i , $i=1,2,\dots$, for the longitudinal and lateral slippery respectively. Taking into account these new state variables, the assumptions can be formulated in a three constraint equations [25]. The longitudinal constraints for the right and left wheels are presented as

$$\dot{\xi}_r = r\dot{\theta}_r - \dot{x}_G \cos \varphi - \dot{y}_G \sin \varphi - b\dot{\varphi} \quad (1-a)$$

$$\dot{\xi}_l = r\dot{\theta}_l - \dot{x}_G \cos \varphi - \dot{y}_G \sin \varphi + b\dot{\varphi} \quad (1-b)$$

The two wheels of the WMR are rigidly connected to the body of the WMR and thus cannot have two different lateral slips. Hence, the two lateral equations have the same expression written as,

$$\dot{\eta} = \dot{\eta}_r = \dot{\eta}_l = \dot{y}_G \cos \varphi - \dot{x}_G \sin \varphi - d\dot{\varphi} \quad (1-c)$$

Note that most of the time the lateral slip may occur along the turning axis of the WMR during cornering. The generalized coordinate vector is defined to be: $q = [x_G, y_G, \varphi, \eta_r, \eta_l, \xi_r, \xi_l, \theta_r, \theta_l]^T$. One can write the above constraint equations in Pfaffian form as, $D(q)\dot{q}=0$, such that

$$S = \begin{bmatrix} -\sin \varphi & \frac{d \sin \varphi - b \cos \varphi}{2b} & \frac{-(b \cos \varphi + d \sin \varphi)}{2b} & \frac{r(b \cos \varphi - d \sin \varphi)}{2b} & \frac{r(b \cos \varphi + d \sin \varphi)}{2b} \\ \cos \varphi & \frac{-(d \cos \varphi + b \sin \varphi)}{2b} & \frac{d \cos \varphi - b \sin \varphi}{2b} & \frac{r(d \cos \varphi + b \sin \varphi)}{2b} & \frac{r(b \sin \varphi - d \cos \varphi)}{2b} \\ 0 & -\frac{1}{2b} & \frac{1}{2b} & \frac{r}{2b} & \frac{-r}{2b} \\ 1 & 0 & 0 & 0 & 0 \\ 1 & 0 & 0 & 0 & 0 \\ 0 & 1 & 0 & 0 & 0 \\ 0 & 0 & 1 & 0 & 0 \\ 0 & 0 & 0 & 1 & 0 \\ 0 & 0 & 0 & 0 & 1 \end{bmatrix} \quad (3)$$

It is assumed that the non-holonomic mobile robot have bounded uncertainties and its estimated dynamics can be described by the equation,

$$\widehat{M}(q)\ddot{q} + \widehat{B}(\dot{q}) = E(q)\tau + F(\ddot{q}) + D^T(q)\lambda \quad (4)$$

$$\widehat{M}(q) = M(q) + \Delta M(q)$$

$$\widehat{B}(\dot{q}) = B(q) + \Delta B(\dot{q})$$

This can be written as

$$D = \begin{bmatrix} \cos \varphi & \sin \varphi & b & 0 & 0 & 1 & 0 & 0 & 0 \\ \cos \varphi & \sin \varphi & -b & 0 & 0 & 0 & 1 & 0 & 0 \\ \sin \varphi & -\cos \varphi & d & 1 & 0 & 0 & 0 & 0 & 0 \\ \sin \varphi & -\cos \varphi & d & 0 & 1 & 0 & 0 & 0 & 0 \end{bmatrix} \quad (1-d)$$

Let $S(q) \in \mathbb{R}^{9 \times 4}$ be a full rank matrix such that columns of $S(q)$ are in the null space of D , and consequently $S(q)$ spans $N(D)$. In this case we can write, $S(q)D(q)=0$. As \dot{q} is in the null space of D there exists a velocity vector v such that [8].

$$\dot{q} = S(q)v \quad (2)$$

Solving the system (1) for the vector $v = [\dot{\eta}, \dot{\xi}_r, \dot{\xi}_l, \dot{\theta}_r, \dot{\theta}_l]$, we obtain the matrix $S(q)$ whose expression is (3).

$$M(q)\ddot{q} + B(\dot{q}) = E(q)\tau + F(\ddot{q}) + \rho(q, \dot{q}, \ddot{q}) + D^T(q)\lambda \quad (5)$$

Such That

$$\rho(q, \dot{q}, \ddot{q}) = -\Delta M(q)\ddot{q} - \Delta B(\dot{q}) \quad (6)$$

Multiplying equation (5) by $S^T(q)$, we get:

$$S^T(q)E(q) \begin{bmatrix} \tau_r \\ \tau_l \end{bmatrix} + S^T(q)F(\ddot{q}) = S^T(q)M(q)\ddot{q} + S^T(q)B(q, \dot{q}) - S^T(q)\rho(q, \dot{q}, \ddot{q}) \quad (7)$$

Such that,

$$M = \begin{bmatrix} m_r & 0 & 0 & 0 & 0 & 0 & 0 & 0 & 0 \\ 0 & m_r & 0 & 0 & 0 & 0 & 0 & 0 & 0 \\ 0 & 0 & I_{rz} + 2I_{wz} & 0 & 0 & 0 & 0 & 0 & 0 \\ 0 & 0 & 0 & m_w & 0 & 0 & 0 & 0 & 0 \\ 0 & 0 & 0 & 0 & m_w & 0 & 0 & 0 & 0 \\ 0 & 0 & 0 & 0 & 0 & m_w & 0 & 0 & 0 \\ 0 & 0 & 0 & 0 & 0 & 0 & m_w & 0 & 0 \\ 0 & 0 & 0 & 0 & 0 & 0 & 0 & I_{wy} & 0 \\ 0 & 0 & 0 & 0 & 0 & 0 & 0 & 0 & I_{wy} \end{bmatrix}; B(\dot{q}) = \begin{bmatrix} 0 \\ 0 \\ 0 \\ m_w \dot{\phi} \dot{\rho}_r \\ m_w \dot{\phi} \dot{\rho}_l \\ -m_w \dot{\phi} \dot{\eta}_r \\ -m_w \dot{\phi} \dot{\eta}_l \\ 0 \\ 0 \end{bmatrix};$$

$$E = \begin{bmatrix} 0 & 0 & 0 & 0 & 0 & 0 & 0 & 1 & 0 \\ 0 & 0 & 0 & 0 & 0 & 0 & 0 & 0 & 1 \end{bmatrix}^T;$$

$$F(\ddot{q}) = [0 \quad 0 \quad 0 \quad f_{latr} \quad f_{latl} \quad f_{longr} \quad f_{longl} \quad -r f_{longr} \quad -r f_{longl}]^T$$

Note that $F(\ddot{q}) \in \mathbb{R}^{9 \times 1}$ is a vector of traction forces. Expression (7) represents the inverse dynamic model of the mobile robot. It helps in elaborating the reference signals to be sent to the motors. We remark that the torques are written in terms of the robot acceleration. However, we are usually interested in controlling the mobile robot in terms of the angular speed and acceleration of the wheels. Thus, a relation between the motor torques and the system parameters can be established.

Deriving equation (2), we obtain

$$\ddot{q} = \dot{S}(q)v + S(q)\dot{v} \quad (8)$$

When substituting \ddot{q} into equation (7) we get:

$$S^T E \tau + S^T(q)F(\ddot{q}) + S^T(q)\rho(q, \dot{q}, \ddot{q}) = S^T(q)M(q)S(q)v + S^T(q)M(q)\dot{S}(q)v + S^T(q)B(q, \dot{q}) \left(-M(q)\dot{S}(q)v - B(\dot{q}) \right) \quad (9)$$

More explicitly, the angular acceleration is written as:

$$\dot{v} = (S^T(q)M(q)S(q))^{-1} S^T(q) (E\tau - M(q)\dot{S}(q)v - B(\dot{q}) + F(\ddot{q}) + \rho(q, \dot{q}, \ddot{q})) \quad (10)$$

3. State space representation

Let x be the state vector such that

$$x = [q \quad v]^T \quad (11)$$

The expression of state variables can be readily obtained as

$$\dot{x} = \begin{bmatrix} \dot{q} \\ \dot{v} \end{bmatrix} = \begin{bmatrix} S(q)v \\ \hat{f}_2 \end{bmatrix} + \begin{bmatrix} [0]_{9 \times 1} \\ (S^T(q)M(q)S(q))^{-1} (S^T E \tau) \end{bmatrix} \quad (12)$$

where

$$\hat{f}_2 = f_2 + \Delta F + \Delta f_2 \quad (13)$$

Such that

$$f_2 = (S^T(q)M(q)S(q))^{-1} S^T(q) \left(-M(q)\dot{S}(q)v - B(\dot{q}) \right) \quad (14)$$

$$\Delta F = (S^T(q)M(q)S(q))^{-1} S^T(q) F(\ddot{q}) \quad (15)$$

$$\Delta f_2 = (S^T(q)M(q)S(q))^{-1} S^T(q) \rho(q, \dot{q}, \ddot{q}) \quad (16)$$

Once the system is put in its state space form, it can be used for the determination of the control law. Let $T = S^T E \tau$, by introducing a new input variable u , T is chosen to be

$$T = S^T(q)M(q)S(q)(u - f_2) - S^T(q)\hat{F}(sr, sa) - S^T(q)\rho(q, \dot{q}, \ddot{q}) \quad (17)$$

In this study, the uncertain term $\rho(q, \dot{q}, \ddot{q})$ is considered to be negligible and the vector of the slipping forces $\hat{F}(sr, sa)$ is obtained from a fuzzy force estimator to compensate the term ΔF , and whose implementation will be given in section 5. If we suppose that $\hat{F}(sr, sa)$ cancels the term $\Delta F(\ddot{q})$ with some tolerable error, then the state equation given by equation (12) can be simplified to

$$\dot{x} = \begin{bmatrix} \dot{q} \\ \dot{v} \end{bmatrix} = \begin{bmatrix} S(q)v \\ [0]_{5 \times 1} \end{bmatrix} + \begin{bmatrix} [0]_{12 \times 2} \\ I_{2 \times 2} \end{bmatrix} u \quad (18)$$

In a more compact form, we can write

$$\dot{x} = f(x) + g(x)u \quad (19)$$

where

$$f(x) = \begin{bmatrix} S(q)v \\ [0]_{5 \times 1} \end{bmatrix},$$

$$g(x) = \begin{bmatrix} [0]_{12 \times 2} \\ I_{2 \times 2} \end{bmatrix}$$

4. Non-singular finite time sliding mode control

Sliding mode control is an interesting mathematical tool when it comes to design control laws that are robust against parameter variation and external disturbances for systems presenting nonlinear terms. The basic idea adopted in this work, is to move the system

trajectories toward the sliding surface in a finite time and remaining on it. The control is achieved through non-singular terminal sliding mode [17, 18]. This technique has attracted many researchers and many theoretical approaches have been developed for different types of mathematical structures. It gives the required mathematical tools to many authors to contribute in obtaining solutions to many complex problems. For our purpose, we choose the reference point P_r that is located in the front of the WMR at a distance L_r from P_G . Hence, the output vector is written as:

$$y = h(x) = \begin{bmatrix} x_d(q) \\ y_d(q) \end{bmatrix} = \begin{bmatrix} x_G + L_r \cos \phi \\ y_G + L_r \sin \phi \end{bmatrix} \quad (20)$$

The time derivative of y yields

$$\dot{y} = \frac{\partial h}{\partial x} \dot{x} = \frac{\partial h}{\partial x} (f(x) + g(x)u) \quad (21)$$

$$\dot{y} = L_f h(x) + L_g h(x)u \quad (22)$$

Since $L_g h(x) = 0$, we compute once more the Lie derivative of equation (21) in order to make the input control u appear in the equation, we obtain

$$\ddot{y} = L_f^2 h(x) + L_g L_f h(x)u \quad (23)$$

Now, a robust control law u that guaranties a fast finite convergence is sought. This can be established using a non-singular terminal sliding mode control (NTSMC) such that

$$-u_{max} \leq u \leq u_{max}.$$

Let the sliding surface s be

$$s = e + \frac{1}{\lambda} |\dot{e}|^{p/q} \text{sign}(\dot{e}) \quad (24)$$

Such that:

$$\begin{cases} \dot{e} = y - y_d \\ \dot{\dot{e}} = \dot{y} - \dot{y}_d \end{cases} \quad (25)$$

The time derivative of the surface s is obtained as,

$$\dot{s} = \dot{e} + \frac{p}{\lambda q} |\dot{e}|^{\frac{p-1}{q}} \ddot{e} \quad (26)$$

Choosing u such that

$$u = -(L_g L_f h(x))^{-1} \left(L_f^2 h(x) + \lambda \frac{q}{p} |\dot{e}|^{(2-\frac{p}{q})} + k \text{sign}(s) - \dot{y}_d \right) \quad (27)$$

u represents the NTSMC control law, and is feasible if determinant of $(L_g L_f h(x)) \neq 0$, and this is true since $L_r \neq d$. In this case

$$\dot{s} = -k \frac{p}{\lambda q} \dot{e}^{\frac{p-1}{q}} \text{sign}(s) \quad (28)$$

Where, k is a diagonal matrix with positive scalars and since p and q are positive odd integers and $1 < \frac{p}{q} < 2$, there is $\dot{e}_i^{\frac{p-1}{q}} > 0$ for $\dot{e}_i \neq 0$ [18], hence stability is ensured. To avoid the undesirable control chattering, the discontinuous sign function $\text{sign}(s)$ is replaced by a continuous saturation function $\text{sat}(s, \Phi)$. The control law in (27) is used to generate the torque vector in (17) in order to minimize the position error of the WMR with respect to the reference trajectory. However, equation (17) contains the term $S^T(q) \hat{F}(sr, sa)$, which includes longitudinal and lateral slipping forces. The forces that appear whenever the motion of the system is accompanied by a longitudinal and/or lateral displacement due to slip are usually unpredictable.

This can cause severe instability. In this work, we use fuzzy logic paradigm to estimate these forces to reduce their effect or in the ideal case eliminate them.

5. Fuzzy logic based slip force estimation

5.1 Problem formulation

When the mobile robot wheels are in contact with the ground, the tyres deflect due to the pneumatic characteristics and the weight exerted by the robot

mechanical structure. These result in forces generated in the contact patch between the tyre and the ground surface. Many attempts were made to give mathematical models to wheel-ground surface interaction. They can be classified into two major categories: empirical models and analytical models [29]. Empirical models are based on curve fitting techniques and can accurately capture the non-linear characteristics of traction forces, but most of these models lack physical interpretation and they cannot directly reflect the effect of some dynamic factors such as hysteresis and tyre pressure. On the other hand, analytical models are represented by differential equations that can model these dynamic factors but lacks the empirical accuracy. Maybe the Delft model notoriously named the "Magic Formula", which is a semi-empirical elegant model based on curve fitting technique, is the most appropriate model that has been widely accepted in industry and academic sector. It was introduced by Bakker, Nyborg & Pacejka in 1987 [30] and since then it has been revised several times [31-33]. It presents several advantages such as correctness, simplicity and the aptitude to be interpreted physically. In fact, this model allows obtaining a representation of the longitudinal and lateral forces as well as that of the self-aligning torque solely from the same equation and a set of six parameters. It should be noted that the slip ratio and the slip angle form the inputs of the formula whereas the other parameters (the vertical load, the camber angle, the tyre adhesion to the ground, the inflation pressure of the tyre) come into the determinations of the macro-coefficients that govern the shape of the curve generated by the Magic Formula. The more general form of the magic formula for a given load and camber angle is as follows

$$y = D \sin \left(C \arctan \left(Bx - E(Bx - \arctan Bx) \right) \right) \quad (29)$$

Such that

$$Y(X) = y(x) + S_v \\ x = X + S_h$$

S_v and S_h introduce a vertical and horizontal offset respectively with respect to the origin. Y can represent the lateral force F_{lat} or the longitudinal

force F_{long} and X can represent either the tyre drift angle δ or the rate of sliding when one seeks to obtain the lateral force or the longitudinal force respectively. The macro coefficients B , C , E and D are the four-macro dimensionless coefficients defined respectively as the stiffness, shape, curvature and peak. However, these macro coefficients depend on the nominal vertical load of the robot F_z on the tyre, and most importantly on the micro parameters, which depend on the soil surface on which the robot is rolling. Their estimation is important and must be accurate in order to predict the forces exerted by the tyres. In practical applications, it is usually difficult to determine these parameters chiefly when the nature of the surface changes. Fuzzy logic based approach as a universal approximate is used in this work to approximate the lateral as well as the longitudinal forces when the mobile robot is subjected to lateral or/and longitudinal slip. Its main advantage is the non-requirement of detailed mathematical model to formulate the needed function, beside its capability to operate for a large range of inputs.

5.2 Determination of lateral and longitudinal forces based on fuzzy rules

When the pure rolling assumption is no more valid, the mobile robot is in face of a new situation where the traction force is relevant. In fact, slip is present whenever the mobile robot navigates with relatively high speed on slippery or irregular surfaces. In order to determine the lateral and

longitudinal forces, fuzzy reasoning could easily find application in such systems. In this work, we assume that the right and left angular speeds $\dot{\theta}_r$ and $\dot{\theta}_l$ as well as the lateral speed of the center of each wheel $\dot{\eta}$ can be measured. The slip is modeled as a slip ratio (sr) and a slip angle (sa) and satisfy the following relations,

$$sr_i = \frac{r\dot{\theta}_i - v_i}{\max(r\dot{\theta}_i, v_i)}, sa = \tan^{-1}\left(\frac{\dot{\eta}}{v}\right) \quad (30)$$

Where v_i is the longitudinal speed of the center of the i -th wheel, v is the WMR forward speed, we suppose that the slips sr_i and sa are bounded by s_R and s_A such that

$$s_R = \sup_t \|sr(t)\|, s_A = \sup_t \|sa(t)\|$$

To get the required forces, the inputs of the fuzzifier are fed with values of the slip ratio and the slip angle. These variables are mapped from the crisp input domain to the fuzzy domain characterized by the six membership functions shown in Figures 2a and 2b. The fuzzy rule base consists of a sequence of linguistic sentences in the form of *If-Then* rules to infer a set of fuzzy outputs represented by five membership functions for the longitudinal and lateral forces as it is depicted in figures 3a and 3b successively.

Tables 1 and 2 show appropriate sets of rules used for extracting the appropriate forces. The crisp values of these forces are obtained using the center-of-gravity defuzzification technique.

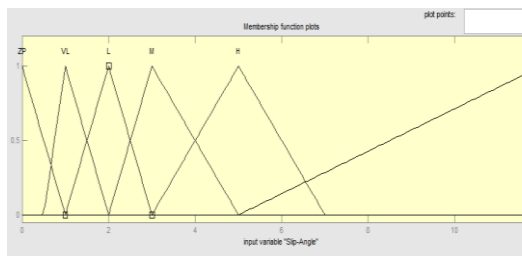


Fig 2a- Slip angle

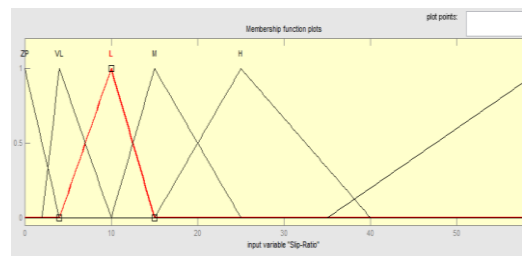


Fig 2b. Slip ratio

Fig 2. Input variables of the fuzzy logic model

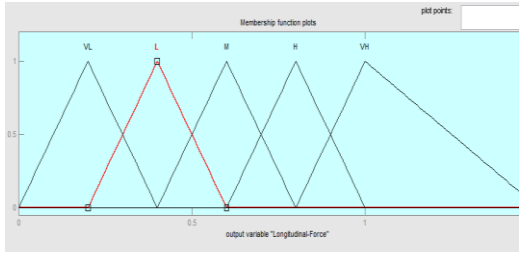


Fig 3a. Longitudinal force

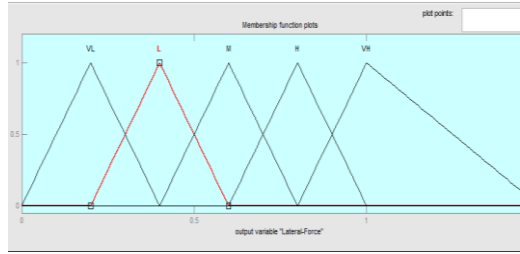


Fig 3b. Lateral force

Fig 3. Output variables of the fuzzy logic model

Table 1. Fuzzy rules for lateral force

Slip Ratio (σ)	Slip Angle (α)					
	ZP	VL	L	M	H	VH
ZP	VL	L	M	VH	VH	VH
VL	VL	L	M	H	VH	VH
L	VL	L	M	H	VH	VH
M	VL	L	M	H	VH	VH
H	VL	L	M	H	VH	VH
VH	VL	L	M	H	H	H

Table 2. Fuzzy rules for longitudinal force

Slip Ratio (σ)	Slip Angle (α)					
	ZP	VL	L	M	H	H
ZP	L	VL	VL	VL	VL	VL
VL	M	M	VH	VL	VL	VL
L	VH	VH	VH	H	M	M
M	VH	VH	VH	H	H	M
H	VH	VH	VH	H	H	M
VH	VH	VH	H	H	H	L

The design of the fuzzy rules is inspired from the resulting curves obtained from Pacejka formula (magic formula) given by equation (29) for different values of slip ratios and slip angles. The curves for a particular type of tyre are depicted in figures 4 and 5, obtained for a normal force $F_z=1.0kN$. The parameters associated with these curves are taken from the reference [34]. The determined forces obtained at the output of the module of defuzzification are scaled by a gain G found proportional to F_z .

$$G = 0.01 * F_z \tag{31}$$

which varies with the weight of the mechanical structure of the mobile robot since $F_z=m_r*g$. Hence, the estimated forces are the outputs of the fuzzy estimator multiplied by the gain G .

$$F = G * \hat{F} \tag{32}$$

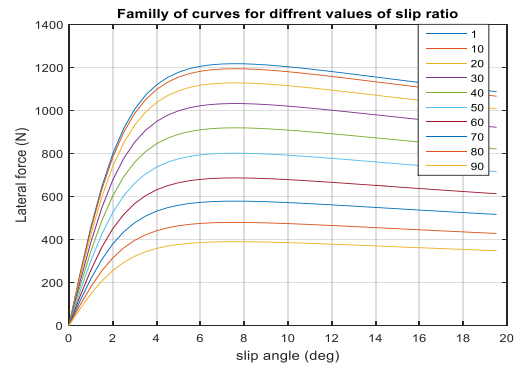


Fig 4. Family of Lateral force curves for different slip ratios

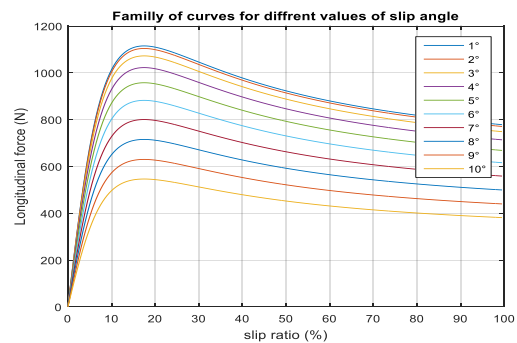


Fig 5. Family of Longitudinal force curves for different slip angles

6. Simulation Results:

To validate the proposed approach, simulation tests are performed to confirm if the wheeled mobile robot succeed in keeping tracking two different types of paths, when part of their surface is made slippery. In each case, we compare the results obtained with and without slippery force compensation. For the simulation task, the WMR parameters (refer to Fig. 1) are as follows: $L_r=0.36m$; $b=0.32m$; $d=0.737m$; $r=0.27m$; $m_r=17kg$; $m_w=0.8kg$;

$$I_{rz}=0.537kgm^2; \quad I_{wy}=0.0023kgm^2;$$

$$I_{wz}=0.0011kgm^2, \text{ the gains are } G=1.7, k=[5 \ 0; \ 0 \ 5].$$

a) Simulation for a straight line path following

1) Without slippery forces compensation.

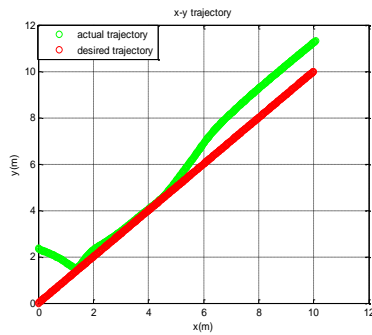


Fig 6a. WMR x-y trajectory

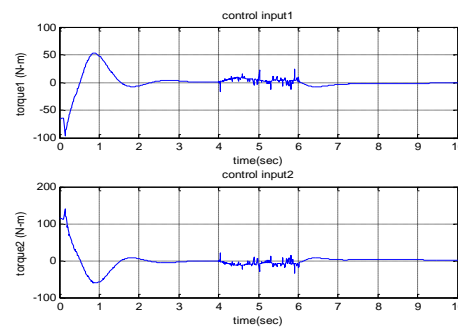


Fig 6b. WMR wheel torques

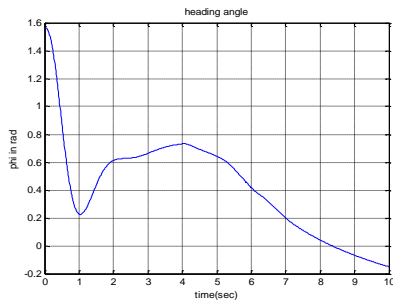


Fig 6c. WMR orientation

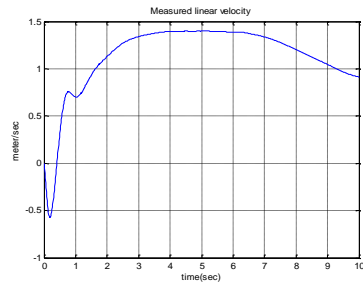


Fig 6d. WMR linear velocity

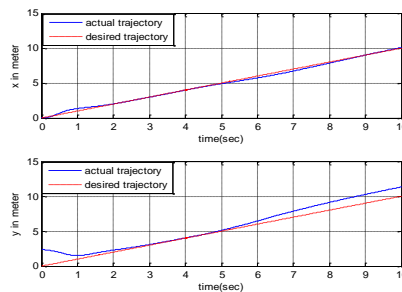


Fig. 6e. WMR x-y configuration

Figs 6. Simulation results for a straight line trajectory tracking without slippery forces compensation

Initially the mobile robot is at position $(x, y, \varphi) = (0, 2, \pi/2)$ and is supposed to follow the straight line: $x=t, y=t$. To highlight slip phenomenon, slip forces are introduced in the dynamic model in the form of a scaled uniformly distributed pseudorandom numbers within the interval 4 to 6 sec.

These forces result in an amount of longitudinal and lateral slip, impacting the robot behavior, which moves away from its reference trajectory.

It results in a bad control despite the robustness of the non-singular terminal sliding mode control, as it is clear from Fig. 6a. Figure 6b depicts the control inputs u_1 and u_2 .

To show the details of the trajectory tracking, we successively reported in Fig. 6c and Fig. 6d the linear velocity plot and the evolution of the heading angle.

Fig. 6c, shows the x and y plots with respect to the running time.

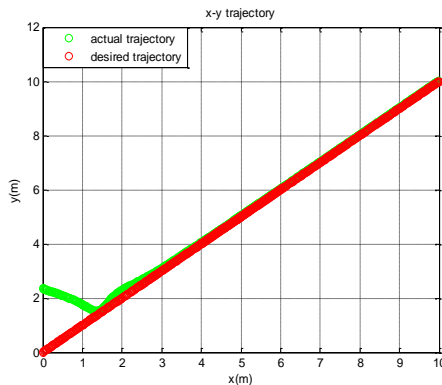


Fig 7a.WMR x-y trajectory

2) With slippery forces compensation.

As described in section 5, the objective is to stabilize the mobile robot to disturbances resulting from tyre slipping. In contrast to the first simulation, where the mobile robot deviates from its path when the slippery affects the mobile robot tyres, the proposed method allows the mobile robot to be invariant to these disturbances. To emphasize the importance of these forces compensation, the designed fuzzy estimator is activated to generate the required forces that reduce the effect of the tyre forces or eliminate them. Computer simulations are conducted in order to validate the proposed scheme. The mobile robot keeps tracking the desired path and seems not to be affected by tyre slips all along the path, as it is shown in Fig. 7a. In Fig. 7b, we report the curves of the actuator outputs τ_1 and τ_2 which are within selected limits τ_{min} and τ_{max} . The remaining figures, Figs. 7c, 7d and 7e, show the details of the trajectory tracking.

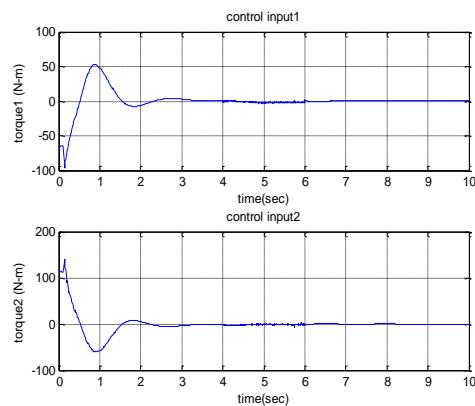


Fig 7b.WMR wheel torques

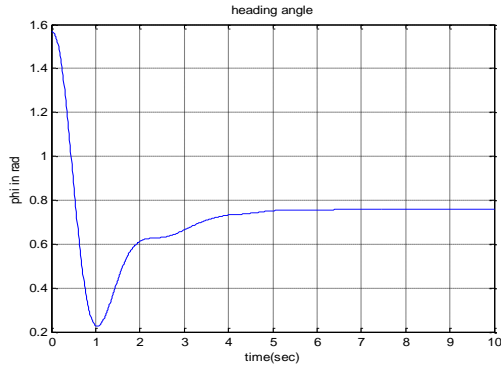


Fig 7c. WMR orientation

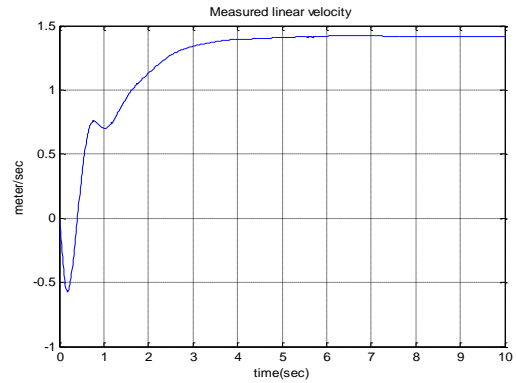


Fig 7d. WMR linear velocity

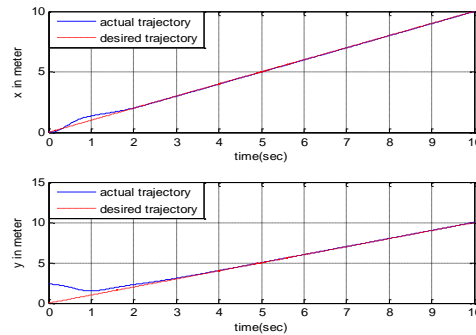


Fig. 7e. WMR x-y configuration

Figs 7. Simulation results for a straight line trajectory tracking with slippery forces compensation

b) Simulation for L-shaped path

The second scenario consists of observing the behavior of the mobile robot when it is asked to follow an L-shaped path. As before, slip forces are introduced in the dynamic model in the form of a scaled uniformly distributed pseudorandom numbers within the interval 4 to 6 sec. It corresponds to a slippery region around the sharp cornering. Initially the mobile robot is at position $(x, y, \varphi) = (0, 0, 0)$. The simulation is replicated for the cases the tyre-forces-estimator is whether activated or not.

1) Without slippery forces compensation.

The simulation carried out on the established model shows that the mobile robot fails in tracking the reference trajectory and deviates away, as it is clear from Fig. 8a. on the other hand, one can have an idea on the efforts developed by the torques by examining Fig. 8b. The remaining figures, Figs. 8c, 8d and 8e, show the degradation of the performances of the system.

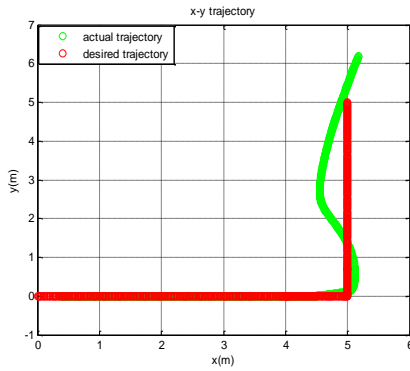


Fig 8a. WMR x-y trajectory

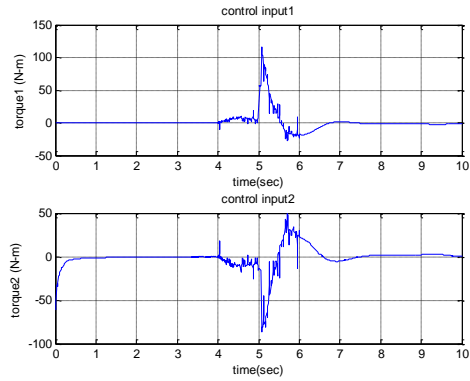


Fig 8b. WMR wheel torques

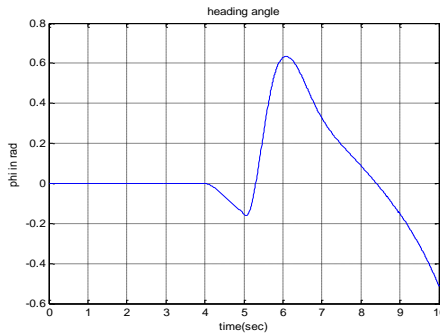


Fig 8c. WMR orientation

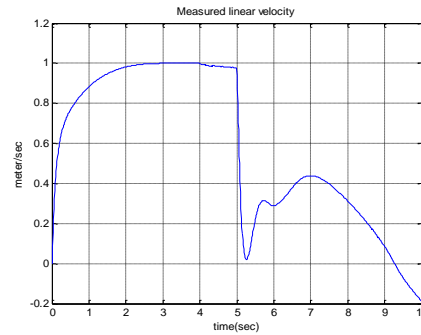


Fig 8d. WMR linear velocity

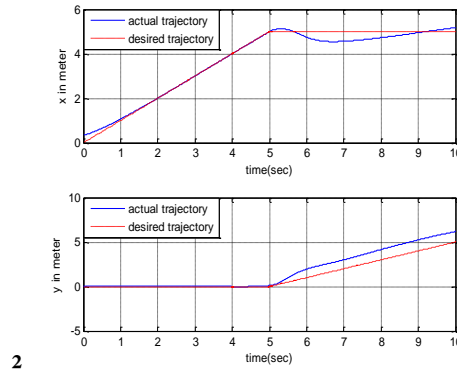


Fig. 8e. WMR x-y configuration

Figs 8. Simulation results for a L-shaped trajectory tracking without slippery forces compensation

2) *With slippery forces compensation.*

When the fuzzy tyre force estimator is activated, the resulting torques, shown in Fig. 9b, succeeded in stabilizing the mobile robot trajectory with negligible slip. The mobile robot is able to respond to the sharp cornering

slipping surface as it is depicted in Fig. 9a. The remaining Figures, 9c, 9d and 9e show the details of the simulation. These curves show clearly the robustness of the approach in conserving the performances of the system in

rejecting the disturbances caused by the tyre slip forces.

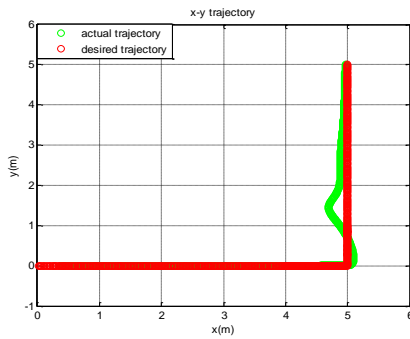


Fig 9a. WMR x-y trajectory

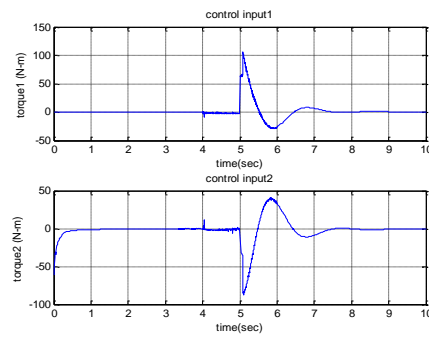


Fig 9b. WMR wheel torques

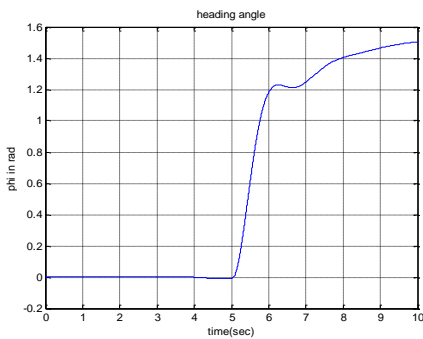


Fig 9c. WMR orientation

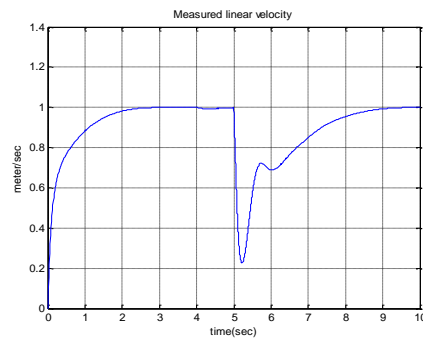


Fig 9d. WMR linear velocity

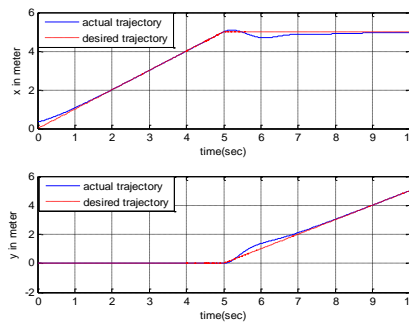


Fig. 9e. WMR x-y configuration

Figs 9. Simulation results for a L-shaped trajectory tracking with slippery forces compensation

7. Conclusion

In this paper, we investigated the possibility of controlling a nonholonomic wheeled mobile robot in maintaining its path while it is subjected to wheel slip. This goal is achieved

by including in the dynamical model the slip dynamics relaxing the assumption of the pure rolling. An association between the nonsingular terminal sliding mode controller and the output feedback control is used to design the control law. The forces that appear

because of wheel slip of the mobile robot moving at high speed or on a slippery surface are compensated using a fuzzy logic based force estimator. It synthesizes the magic formula for a large model of tyres. Simulation results are presented to validate the presented approach. In this paper, we are not pretending that the proposed approach is better than the already existing methodologies. However compared with others e.g., [25], [27], we can affirm that it is simpler and avoids the complexity of the mathematical expressions used in determining the control laws. It gives on the other hand another issue compared to the techniques used to evaluate the parameters that fit the values of the magic formula. We believe that the proposed methodology can as well be applied to autonomous driving cars to overcome the problem of skidding and slipping.

References

- [1] B. d'Andrea-Novet, G. Bastin, and G. Campion. "Modeling and control of non holonomic wheeled mobile robots", In Proceedings of 1991 *IEEE Int. Conf. on Robotics and Automation*, pp.1130-1135, Sacramento, CA, April 1991
- [2] J. P. Laumond, S. Sekhavat and F. Lamiroux, "Guidelines in nonholonomic motion planning for mobile robots", (pp. 1-53), *Springer Berlin Heidelberg*, 1998.
- [3] Y. Zhuang, Y. Liu, W. Wang, Z. Zhan, "Hybrid path planning for nonholonomic mobile robot based on steering control and improved distance propagating", *Int. Conf. on Modeling, Identification and Control (ICMIC)*, pp. 704 – 709, Okayama, Japan, 2010
- [4] Frazzoli, Emilio, Munther A. Dahleh, and Eric Feron. "Real-time motion planning for agile autonomous vehicles", *Journal of Guidance, Control, and Dynamics* 25.1, pp. 116-129, 2002.
- [5] C. Samson and K. Ait-Abderrahim. "Feedback stabilization of a nonholonomic wheeled mobile robot", *In Proc. 8 of the Int. Conf. on Intelligent Robots and Systems (IROS)*, 1991.
- [6] A. Isidori, *Nonlinear Control Systems*, Springer, 3rd Ed. -1995.
- [7] N. Sarkar, X. Yun, and V. Kumar, "Dynamic Path Following A New Control Algorithm for mobile Robots", *Proc. of the 32nd IEEE Conf. on Decision and Control*, 3, 2670-2675, San Antonio, Texas, Dec. 1993.
- [8] X. Yun and Y. Yamamoto, "Internal dynamics of a wheeled mobile robot", *Proc. of the IEEE/RSJ Int. Conf. on Intelligent Robots and Systems, IROS*, Vol.2, pp. 1288-1294, 1993.
- [9] V. Utkin, "Variable structure systems with sliding modes", *IEEE Trans. on Automatic Control*, Vol. 22, issue 2, pp. 212-222, 1977.
- [10] H. R. Ramirez, Variable structure control of non-linear systems, *Int. J. System Sci.*, Vol.18, no. 9, pp. 1673-1689, 1987.
- [11] H.S. Shim, J. H. Kim; K. Koh, "Variable structure control of nonholonomic wheeled mobile robot", *Proc. of the IEEE Int. Conf. on Robotics and Automation*, Vol. 2 pp. 1694-1699, 1995.
- [12] Y. Wu, X. Yu, Z. Man, "Terminal sliding mode control design for uncertain dynamic systems", *Systems & Control Letters* 34, pp. 281-287, 1998
- [13] M. Zhihong, A. P. Paplinsky and H. R. Wu, A robust MIMO terminal sliding mode control scheme of rigid manipulators, *Automatica*, Vol. 38, Issue 12, pp. 2159=2167, Dec. 2002.
- [14] S. Yua, X. Yub, B. Shirinzadehc and Z. Mand, "Continuous finite time control for robotic manipulators with terminal sliding mode", *Automatica*, Vol.41, no. 11, pp.1957-1964, nov. 2005.
- [15] C. L. Chen, C. W. Chang and H. T. Yau, "Terminal sliding mode control for aeroelastic systems", *Jour. of Nonlinear Dynamic*, Springer, Vo. 38, no. 12, pp. 2015-2026, Nov. 2012.
- [16] Y. Feng, X. Yu, Z. Man, "Non-singular terminal sliding mode control of rigid manipulators", *Automatica*, Vol. 38, Issue 12, pp. 2159–2167, Dec. 2002.
- [17] S. Y. Chen and F. J. Lin, "Robust nonsingular terminal sliding-mode control for nonlinear magnetic bearing system," *IEEE Trans. Control Syst. Technol.*, vol. 19, no. 3, pp. 636–643, May 2011.
- [18] Y. Feng, X. Yu, F. Han, "On nonsingular terminal sliding-mode control of nonlinear systems", *Automatica*, Vol. 49, Issue 6, pp. 1715–1722, June 2013.
- [19] T. Binazadeha and M.H. Shafieia, "Nonsingular terminal sliding-mode control of a tractor-trailer system", *Systems Science & Control Engineering: Taylor & Francis*, Vol. 2, pp. 168–174, 2014.
- [20] D. Zhao, S. Li, Q. Zhu, "Output feedback terminal sliding mode control for a class of a second order nonlinear systems", *Asian Journal of control*, *Wiley Online Library*, Vol. 15, No. 1, pp. 1-11, Jan. 2013.
- [21] S. Ding, W. X. Zheng, "Nonsingular terminal sliding mode control of nonlinear second-order systems with input saturation", *Int. J. Robust Nonlinear Control*, 26: 1857-1872, 2016.

- [22] P. S. Londhe, D. D. Dhadekar, B. M. Patre, L. M. Waghmare, "Non-singular Terminal sliding mode control for robust trajectory tracking control of an autonomous underwater vehicle", *IEEE Indian Control Conference (ICC)*, 4-6 Jan. 2017, Guwahati, India.
- [23] R. Balakrishna and A. Ghosal, "Modeling of slip for wheeled mobile robots", *IEEE transactions on Robotics and Automation*, 11(1):126-132, 1995.
- [24] L. Garcia and J. Tornero, "Kinematic modeling of wheeled mobile robots with slip", *Advanced Robotics*, Taylor & Francis, V. 21, No. 11, pp. 1253-1279, 2007
- [25] N. Sidek and N. Sarkar, "Dynamic modeling and control of nonholonomic wheeled mobile robot subjected to wheel slip", *PhD thesis*, Vanderbilt University, 2008.
- [26] Y. Tian and N. Sarkar, "Formation control of mobile robots subjected to wheel slip", *In IEEE International Conference on Robotics and Automation (ICRA)*, pp. 4553-4558, 2012.
- [27] Y. Tian, N. Sarkar, "Control of a mobile robot subject to wheel slip", *J. Intell. Robot Syst.*, Springer, V. 74, issue 3-4, pp.915-929, June 2014.
- [28] R. Jayachandran, S. D. Ashok, S. Narayanan, "Fuzzy logic based modeling and simulation approach for the estimation of tyre forces", *Int. conf. on design and Manufacturing, (IConDM)*, Procedia Engineering 64, pp. 1109-1118, 2013.
- [29] L. Li and F. Y. Wang, "Advanced motion control and sensing for intelligent vehicles," *Springer Science & Business Media*, 2007.
- [30] E. Bakker, L. Nyborg and H. B. Pacejka, "Tyre modeling for use in vehicle dynamics studies," *SAE technical paper* No. 870421, 1987.
- [31] E. Bakker, H. B. Pacejka and L. Linder, "A new tyre model with an application in vehicle dynamics studies," *SAE technical paper* No. 890087, 1987.
- [32] H. B. Pacejka and E. Bakker, "The magic formula tyre model: Tyre-model," *Proc. of 1st Int. Colloquium on tyre models for vehicle dynamics analysis*, pp. 1-18, Netherlands, 1991.
- [33] H. B. Pacejka and I. J. M. Besselink, "Magic formula tyre model with transient properties," *Vehicle system dynamics*, 27(S1), 234-249.
- [34] G. Genta, "Motor Vehicle Dynamics: Modeling and Simulation," *Word Scientific Pub Co Pte. Lmd*, 1997, ISBN 9810229119.